Expression, Purification and Characterization of Enoyl-ACP Reductase II, FabK, from *Porphyromonas gingivalis*

Kirk E. Hevener*, Shahila Mehboob, Teuta Boci, Kent Truong, Bernard D. Santarsiero, and Michael E. Johnson

Center for Pharmaceutical Biotechnology, University of Illinois at Chicago, 900 S. Ashland Ave., Chicago, IL 60607-7173 (USA)

*To whom correspondence should be addressed. Phone: 312-996-5388. Fax: 312-413-9303. E-mail: khevener@uic.edu

Abbreviations: ACP, acyl carrier protein; FAS, fatty acid synthase; NADH, nicotinamide adenine dinucleotide; NADPH, nicotinamide adenine dinucleotide phosphate; IPTG, isopropyl β-D-1-thiogalactopyranoside; FMN, flavin mononucleotide; OTG, n-octyl beta-D-thioglucopyranoside; PgFabK, *Porphyromonas gingivalis* FabK; SpFabK, *Streptococcus pneumoniae* FabK

Abstract

The rapid rise in bacterial drug resistance coupled with the low number of novel antimicrobial compounds in the discovery pipeline has led to a critical situation requiring the expedient discovery and characterization of new antimicrobial drug targets. Enzymes in the bacterial fatty acid synthesis pathway, FAS-II, are distinct from their mammalian counterparts, FAS-I, in terms of both structure and enzymatic mechanism. As such, they represent attractive targets for the design of novel antimicrobial compounds. One such enzyme, enoyl-acyl carrier protein (ACP) reductase II, FabK, is a key, rate-limiting enzyme in the FAS-II pathway. The bacterial organism, *Porphyromonas gingivalis*, is a causative agent of chronic periodontitis that affects up to 25% of the U.S. population and incurs a high national burden in terms of cost of treatment. *P. gingivalis* expresses FabK as the sole enoyl reductase enzyme in its FAS-II cycle, which makes this a particularly appealing target with potential for selective antimicrobial therapy. Herein we report the molecular cloning, expression, purification and characterization of the FabK enzyme from *P. gingivalis*, only the second organism from which this enzyme has been isolated. Characterization studies have shown that the enzyme is a flavoprotein, the reaction dependent upon FMN and NADPH and proceeding via a Ping-Pong Bi-Bi mechanism to reduce the enoyl substrate. A sensitive assay measuring the fluorescence decrease of NADPH as it is converted to $NADP^+$ during the reaction has been optimized for high-throughput, 384-well format. Finally, protein crystallization conditions have been identified which led to protein crystals that diffract x-rays to high resolution.

Keywords: *Porphyromonas gingivalis*, FabK, enoyl-ACP reductase II, purification, characterization, crystallization

Introduction

Chronic or persistent infections are responsible for extensive morbidity and a high burden in terms of costs of illness in the U.S. and worldwide. These infections are typically characterized by the ability of the infecting organism to bypass the host's immune response and may persist for extensive periods, up to the lifespan of the host. Examples of chronic infections that are responsible for large health care costs globally include HIV, hepatitis, and tuberculosis. Another example is chronic periodontitis, an inflammatory destruction of the bone and tooth-supported tissues associated with polymicrobial infection. Periodontitis is the major cause of tooth loss in the world, and is considered the most common adult infection [1]. It has been estimated that the national cost of treating periodontal diseases, including gingivitis and periodontitis, exceeds 5 billion dollars; with periodontitis being the major contributor to this estimate [2, 3]. Although an estimated 750 different bacterial species reside in the human mouth, periodontitis has been attributed to less than 5% of these organisms [3, 4]. The bacterial species *Porphyromonas gingivalis* is associated with a particularly aggressive, chronic disease that is often resistant to standard treatments [5-8]. Recent studies have shown that *P. gingivalis* is a keystone species that can accelerate the disease progression by disrupting the host-microbial homeostasis in these polymicrobial infections [9]. These studies have revealed that disruption of the host complement system is a possible mechanism by which *P. gingivalis* is able to facilitate chronic periodontal infection. This implies that targeting *P. gingivalis* for specific antimicrobial therapy may have a broad, clinical impact on community-wide oral health. Because *P. gingivalis* is frequently resistant to standard treatments, there is a critical need to develop novel treatments targeting previously unexploited pathways [10, 11].

One attractive, yet largely unexploited area of antimicrobial research is the bacterial fatty acid synthesis pathway, FAS-II. This pathway is absent in mammals and is essential in Gram-negative bacteria making it an appealing and potentially selective antibacterial target. Although novel, the use of agents targeting the FAS-II pathway in the prevention and treatment of infectious disease is well precedented. The antibacterial triclosan, a known inhibitor of FabI (enoyl-ACP reductase I), has been used as a component of oral hygiene products for some time [12, 13]. Other FabI inhibitors include isoniazid, which targets *Mycobacterium tuberculosis* and is currently approved for use in the U.S. and AFN-1252, a *Staphylococcus aureus* active agent currently in clinical trials [14, 15] . Unfortunately, *P. gingivalis* expresses an isozyme of FabI, FabK (enoyl-ACP reductase II) that is completely resistant to

triclosan and other FabI active agents [16]. FabK falls within a separate category of oxidoreductase enzymes and is structurally and mechanistically distinct from FabI [16]. FabK was first identified by Heath and coworkers in 2000 as a triclosan resistant variant of FabI in *Streptococcus pneumoniae* [17]. It was subsequently isolated and characterized as a flavoenzyme, dependent upon FMN and NADH in a reaction that proceeded via a ping-pong enzymatic mechanism [16, 18]. Since that time, two additional enoyl-reductase isozymes have been identified, FabL and FabV, which have also shown low levels of susceptibility to triclosan [19, 20].

Although the existence of multiple isozymes precludes the possibility of developing broad spectrum antimicrobials targeting enoyl reductase, there is an advantage in that fairly specific antibacterial agents may be developed that target harmful bacterial species, such as *P. gingivalis*, while avoiding activity against the so called 'beneficial bacteria'. The FabK enzyme in *P. gingivalis* presents an interesting possibility to target an aggressive bacterial species associated with chronic periodontitis while causing little disruption to the normal bacterial flora of the oral cavity. As a case in point, *Streptococcus mutans*, the principle organism associated with dental caries, is also FabK dependent while the Lactobacilli, which are considered beneficial, express FabI. Herein, we report the cloning, expression, purification and kinetic characterization of the FabK enzyme from *P. gingivalis*, the second bacterial species, following *S. pneumoniae*, from which this enzyme has been isolated. We present the design and optimization of a fluorescence intensity assay for use in low volume, high-throughput screening campaigns for inhibitory compounds. Finally, crystallization screens are discussed that have identified conditions leading to the production of *P. gingivalis* FabK crystals that diffract to high resolution.

Material and Methods

Reagents, chemicals, biologicals, and equipment

The PCR reagents (PCR SuperMix High Fidelity), restriction enzymes *Bam* HI and *Nde* I, DNA amplification cell line (XL1-Blue), and media (Terrific broth, Luria-Bertani broth) were obtained from Invitrogen Life Technologies (Grand Island, NY). The protein expression cell line, BL21-Gold (DE3), catalog #230132, was obtained from Agilent Technologies (Santa Clara, CA). The QIAquick PCR Purification Kit and QIAprep Spin Miniprep Kit were obtained from QIAGEN (Valencia, CA). Quick Ligation Kit (M2200L) was obtained from New England BioLabs, Inc. (Ipswich, MA). The pET-15b plasmid vector was obtained from Novagen/Millipore (Madison, WI). Genomic DNA (*Porphyromonas gingivalis* strain W83, BAA-308D-5) was obtained from ATCC (Manassas, VA). Oligonucleotide primers were

obtained from Integrated DNA Technologies (IDT, Coralville, IA). The IMAC-Ni column (HisTrap HP, 5 mL) and gel filtration column (HiLoad 26/600 Superdex 200, volume 320 ml, dimensions 26 x 600 mM) were obtained from GE Healthcare (Piscataway, NJ). Ampicillin, n-octyl beta-D-thioglucopyranoside (OTG), isopropyl β-D-thiogalactopyranoside (IPTG), β-nicotinamide adenine dinucleotide 2′-phosphate reduced tetrasodium salt (NADPH), crotonyl coenzyme A trilithium salt (2-butenoyl-CoA) were obtained from Sigma-Aldrich Chemicals (St. Louis, MO). Crystallization screening kits (SaltRx, Index, Crystal Screen, PEG/Ion) and supplies were obtained from Hampton Research (Aliso Viejo, CA).

Plasmid Construction

Genomic DNA isolated from the *P. gingivalis* strain W83 (virulent) was used as the template for amplification of the *fabK* gene (**GenBank ID: AE015924**) [21]. The forward primer 5'-GAA TAA GCA TAT GAA TAG AAT TTG CGA ATT ATT GGG T-3' and reverse primer 5'-AGA TGG ATC CTC ATA TCT CAG TGG G-3' were based upon the sequence of the *fabK* gene (NCBI Gene ID: 2551749, Locus tag: PG1416) and designed to introduce restriction sites for *Bam* HI and *Nde* I. The PCR amplification was performed in 50 µL volume containing 45 µL PCR SuperMix, 1 µL of each primer (roughly 200 µM each), 1 µL template DNA (200 ng), and 2 µL H_2O. The PCR reaction was performed using 30 cycles of denaturation at 95 ˚C (30 seconds), annealing at 54 ˚C (30 seconds), and extension at 68 ˚C (60 seconds). The PCR product was gel extracted using the QIAquick PCR Purification Kit and visualized on a 1% agarose gel stained with ethidium bromide (Figure 1). The purified PCR product was digested with *Bam* HI and *Nde* I to obtain cohesive ends and ligated to digested plasmid expression vector, pET-15b, using the BioLabs Quick Ligation Kit. The ligated vector was transformed by 45-second heat shock (at 42 ˚C) into XL1-Blue competent cells for plasmid amplification. The transformed cells were plated on agarose containing 100 µg/mL ampicillin and grown overnight at 37 ˚C. Plasmid DNA was extracted from selected colonies using the QIAprep spin Miniprep Kit and the sequence of the cloned gene was confirmed by DNA sequencing. A sequence confirmed clone was then selected and transformed, as discussed above for XL1-Blue, into BL21 (DE3) competent cells for expression and purification of the full-length protein. BL21 (DE3) pLysS cells were not used in these studies.

Expression and purification of recombinant PgFabK

To identify the optimal IPTG concentrations and induction times to be used in large-scale protein expressions, a protein mini-expression study was performed. A single colony of BL21 (DE3) cells containing the expression construct was inoculated into a 5-mL Luria-Bertani (LB) broth containing 100 µg/mL ampicillin and incubated overnight at 37 ˚C. The overnight culture was then used to inoculate 3 x

10 mL (0.05 - 0.1 OD_{600}) Terrific Broth (TB) containing 100 µg/mL ampicillin and grown at 37 ˚C, shaking, until the OD_{600} reached approximately 0.6. The three samples were split into duplicates for use as un-induced controls. The cultures were then induced with 0.25 mM, 0.5 mM, and 1 mM IPTG, respectively, and growth was continued up to 6 hours. 1-mL samples were collected from each of the six cultures (3 induced, 3 un-induced) at the zero, 1 hour, 2 hour, 4 hour, and 6 hour time points, and spun down using a microcentrifuge at maximum speed for 5 minutes, followed by removal of the supernatant. The pellets were re-suspended in 30 µL of lysis buffer A (1% OTG in 20 mM Tris-HCl pH 8.0, 0.5 M $MgCl_2$, 1 mg/mL lysozyme, 5 mg DNase, and 1 mM protease inhibitor cocktail) and allowed to sit for 5 minutes, followed by micro-centrifugation at maximum speed for 5 minutes. The supernatant was separated into a clean microfuge tube (soluble fraction) and saved while the pellet was washed by an additional re-suspension in lysis buffer A and micro-centrifugation at maximum speed for 5 minutes. The pellet was re-suspended in equal parts (30 µL each) lysis buffer A and SDS NuPage dye, vortexed for 30 seconds, and then micro-centrifuged at maximum speed for 5 minutes. The supernatant from this step was separated into a clean microfuge tube and saved (insoluble fraction). The optimum induction time and IPTG concentration were obtained by analysis of the samples' target protein content using SDS-PAGE for each of the IPTG concentrations and sample collection times for both the soluble and insoluble fractions (Figure 2).

For large-scale expression and purification, 3 x 10 mL LB broth containing 100 µg/mL ampicillin were inoculated with expression construct harboring cells and allowed to grow overnight at 37 ˚C. The overnight cultures were then transferred into 3 x 500 mL TB broth containing 100 µg/mL ampicillin in 2-liter flasks and grown at 37 ˚C with shaking until the OD_{600} reached approximately 0.6. The cells were induced with 0.5 mM IPTG and growth was continued for 4 hours at 37 ˚C with continuous shaking. The cells were then harvested by centrifugation at 10,000*g* for 15 minutes. After the supernatant was discarded, the cells were stored frozen at -80 ˚C and thawed. The thawed cell pellet was suspended into 15 mL lysis buffer B (50 mM Tris-HCl pH 8.0, 100mM NH_4Cl, 1mg/mL lysozyme, 0.1% Triton X-100, 1 mM DTT, 5 mg DNase, and 1 mM protease inhibitor cocktail) per gram of wet weight cells, stirred under refrigeration at 4 ˚C for one hour, and then lysed by sonication for 10 minutes (0.9 sec on, 0.6 sec off, 65% amplitude). The crude lysate was clarified by centrifugation at 10,000*g* for 15 minutes and the supernatant filtered. The clarified extract was then loaded onto a 5-mL HisTrap HP nickel column equilibrated with binding buffer (50mM Tris-HCl pH 8.0, 100 mM NH_4Cl, and 10 mM imidazole) and the column was washed with two column volumes (10 mL) of binding buffer. The target protein, FabK, was eluted from the column using stepwise gradients of increasing concentrations (5% increments, 4 column

volumes each) of elution buffer (50 mM Tris-HCl pH 8.0, 100 mM NH_4Cl, and 500 mM imidazole). The purity of the collected protein was checked using SDS-PAGE gel electrophoresis and the activity of the target enzyme was confirmed by following a decrease in NADPH UV absorption at 340 nm, as discussed below. The fractions containing the eluted target protein, FabK, were collected and concentrated (using a spin column) to 10 mL volume and then loaded onto a GE Superdex 200 HiLoad gel filtration column that had been equilibrated with running buffer (10 mM MOPS pH 7.5, 100 mM NH_4Cl, 2 mM DTT). The FabK containing fractions that were eluted from the gel filtration column were checked for purity and activity as discussed above, pooled, and concentrated to 5 mg/mL with 30% glycerol added as cryoprotectant. The protein stock was aliquoted, flash frozen in liquid nitrogen, and stored at -30 ˚C. Protein concentrations during purification were determined using the Bradford assay with bovine serum albumin (BSA) as the protein standard [22].

Enzymatic assay and kinetics

All studies have been performed using the oligo-histidine-tagged enzyme. As previously reported, FabK is an FMN dependent oxidoreductase that acts to reduce the enoyl substrate using NADH as the hydride donating cofactor [16]. The activity of the enzyme can be followed by monitoring a decrease in the UV absorption or fluorescence of the NADH cofactor as crotonyl-CoA is converted to butyryl-CoA. NADH (and NADPH) absorb UV light at a wavelength of 340 nm and fluoresce at 460 nm. UV absorption in 1-ml cuvettes was used to check the activity of the enzyme in fractions during purification using a NanoDrop 2000c UV-Vis spectrophotometer. NADPH was used as the cofactor in *P. gingivalis* FabK assays because the enzyme was found to have very low activity in the presence of NADH (see Results and Discussion below). 100 mM NH_4Cl was added to all chromatography, lysis, storage, and assay buffers as this salt had been previously reported to be essential for *S. pneumoniae* FabK stability and activity [16]. During purification, the enzyme was assayed in 50 mM MOPS pH 7.5, with 100 mM NH4Cl. 10-µL protein samples were used during purification assays with 50 µM NADPH and 50 µM crotonyl-CoA (see Table 1). We note that these concentrations are sufficient to gauge enzyme activity in chromatography fractions, but are not optimized for inhibitor screening.

In order to identify balanced assay conditions for the future screening of potential inhibitors, it was necessary to determine the Km values of the NADPH cofactor and the crotonyl-CoA substrate. Detailed enzyme kinetics experiments were performed using varying concentrations of NADPH and crotonyl-CoA. A 1.5-fold serial dilution of NADPH, from 200 µM to 3.6 µM, and 0 µM were tested at 100 µM crotonyl-CoA and a 1.5-fold dilution range of concentrations of crotonyl-CoA, from 1000 µM to 39 µM, and 0 µM were tested at 50 µM NADPH. All assays were performed, in triplicate, at 25 ˚C in

Corning® 384-well, low volume, black, round-bottom assay plates at 10 µL final volume. Fluorescence (excitation wavelength 340 nm, emission 460 nm) was monitored at 30 second intervals using an EnVision Multilabel plate reader. All assays were performed using 30 nM PgFabK enzyme in 50 mM MOPS pH 7.5 with 100 mM NH_4Cl. The reaction is initiated by the addition of the NADPH cofactor. Kinetic constants were estimated by fitting the assay data (slopes calculated from linear portion of RFU vs. time plots) to equations (1) or (2) using the program, OriginPro v8.6:

$$v = \frac{V_{max} \times [S]}{Km + [S](1 + [S]/Ki)} \quad (1)$$

$$v = \frac{V_{max} \times [S]}{Km + [S]} \quad (2)$$

where V_{max} is the maximum velocity, [*S*] is concentration of the varied substrate (NADPH or crotonyl-CoA), *Km* is the Michaelis constant for the varied substrate, and *Ki* is the inhibition constant defining substrate inhibition (see Results and Discussion).

Protein Crystallization

To identify optimal crystallization conditions for high-resolution x-ray crystallography studies, a series of sparse-matrix screens using commercially available crystallization kits were manually prepared using the hanging drop, vapor diffusion method in 24-well crystallization plates. The following kits were screened at 25 ˚C and 4 ˚C, using 0.5 mL well volume of crystallization solution: SaltRx, Index, Crystal Screen, and PEG/Ion (obtained from Hampton Research). Two trial drops per well, one containing only protein and one containing protein with 5 mM NADPH were mixed with an equal amount of well solution (1:1, 2 µL each). The stock protein solution used in the crystallization trials was concentrated to 5 mg/mL in 10 mM MOPS, pH 7.5 with 100 mM NH_4Cl, and 5 mM DTT; which resembled the conditions previously reported in the crystallization of the *S. pneumoniae* FabK enzyme [23]. The crystallization studies used the oligo-histidine-tagged protein at a purity estimated (by SDS-PAGE, see below) to be greater than 98%.

Following the identification of initial crystallization conditions (see Results and Discussion below); a microseeding trial was performed in an attempt to improve the diffraction of the initial crystal hits. A series of 10-fold dilution stock microseeding solutions were prepared using the Seed Bead™ kit from Hampton Research. A crystal was harvested from fine screens performed around the initial hit

condition (PEG/Ion #46, 25 ˚C) and placed into a microcentrifuge tube containing 50 µL of the well solution. The tube was vortexed for 60 seconds and the solution diluted with an additional 450 µL of well solution, giving the initial dilution from which four further dilutions (1:10) were prepared. A crystallization trial using the same hit condition with the seed stock dilutions was performed to identify the optimum dilution for subsequent sparse-matrix screens with microseeding. For microseeding trials, 1 µL of the second dilution, 1:10, was added to each drop (total 5 µL), prepared as discussed above, for the screening kits: SaltRx, Index, Crystal Screen, and PEG/Ion. Microseeding crystallization trials were performed at 25 ˚C only.

Results and Discussion

Cloning and Expression of recombinant PgFabK

The *fabK* gene from *P. gingivalis*, strain W83 (NCBI Gene ID: 2551749, Locus tag: PG1416) comprises a total length of 942 base pairs and encodes a 313 residue product with a mass of 33.09 kilodaltons [21]. To overexpress the target protein, FabK, the *fabK* gene was cloned into the *Bam* HI and *Nde* I restriction sites of the pET-15b plasmid vector, a T7*lac* promoted vector carrying an N-terminal His_6-tag with a thrombin cleavage site and ampicillin resistance determinant. Upon confirmation of the cloned gene by DNA sequencing, the plasmid was transformed into *E. coli* strain BL21 (derivative 3) for overexpression of the FabK protein. Cloning and transformation proceeded with little difficulty.

To test the expression levels of FabK and identify an optimum concentration of IPTG to use for induction as well as the optimal cell growth time after induction, samples from the cultures of a protein mini-expression after induction were collected and analyzed by SDS-PAGE. Three different concentrations of IPTG were used, 0.25 mM, 0.5 mM, and 1 mM, with un-induced controls for each, and samples were collected at 0, 1, 2 , 4 and 6 hours for each. Soluble and insoluble fractions were collected as discussed above and the relative levels of protein expression were analyzed using gel electrophoresis. The greatest expression levels of soluble protein were seen using 0.5 mM IPTG induction and 4 hours of cell growth, with no significant increase at 6 hours (Figure 2). Therefore, for large scale production of the PgFabK protein, the cell cultures were induced with 0.5 mM IPTG and the induction time was limited to 4 hours. Although a significant amount protein was noted in the insoluble fraction, roughly equal to the soluble fraction, the soluble portion was estimated to be of sufficient yield (see purification discussion below) to fulfill the needs of our future drug discovery efforts, including enzyme assays and crystallography trials. Therefore no attempts have been made to date to collect the insoluble protein or further optimize the FabK expression. We note the appearance of a large band at approximately 12 kDa,

visible in both the mini-expression (Figure 2) and large-scale expression (Figure 3), which we believe to be the lysozyme enzyme (14 kDa). As mentioned in the Methods section above, lysozyme was used in both lysis buffers at a concentration of 1mg/ml.

Purification of recombinant PgFabK

Table 1 shows the results of a typical PgFabK protein purification, including activity, purity and yield for each step. The purification of the PgFabK protein was performed using two chromatographic steps: immobilized metal ion affinity (IMAC) using a nickel chelate column with affinity for the polyhistidine-tagged protein, followed by gel filtration chromatography using a HiLoad™ Superdex™ column (Figure 3). The PgFabK target protein elution from the Ni IMAC column began at 15% Buffer B (elution buffer), which was at 83.5 mM imidazole concentration. PgFabK elutes from the gel filtration column as an active monomer. The FabK enzyme is a flavoprotein which is clearly visible in collected fractions due to its bright yellow color (oxidized FMN). Colored fractions collected from each purification step were further analyzed by SDS-PAGE and for enzymatic activity as discussed above. The purity of the protein after the first chromatography step (estimated 90%) is sufficient for enzyme assay of potential inhibitors, but insufficient for crystallography trials; hence the second step of purification. The estimated purity of the PgFabK protein after the second chromatographic step is greater than 98% (Figure 3). In Figure 3, we note the appearance of a large band at 66 kDa in lane 7 (pooled Ni column protein fractions), which we believe is the protein dimer. The appearance of this dimer band on a gel run under denaturing conditions is interesting, and is probably indicative of oxidation of the protein (and subsequent dimerization) on the gel. This hypothesis is supported by the disappearance of the dimer band when the reducing agent, beta-mercaptoethanol was added to the sample buffer. The purification protocol has been performed several times to date, with an average yield after two steps of purification of 10 - 15 mg per liter of culture media (1.2 - 1.9 mg of purified protein per gram of wet weight cells). The gel filtration running buffer (10 mM MOPS pH 7.5, 100 mM NH_4Cl, 2 mM DTT) was selected so that the final protein product would be collected in buffer conditions suitable for crystallography trials (see discussion below). These conditions are also used as storage buffer, with 30% glycerol added as cryoprotectant. The activity of the PgFabK protein after storage at -30 ˚C for 4 months has been confirmed by enzyme assay.

The PgFabK enzyme is surprisingly stable. There is no significant loss of enzymatic activity after one month storage under refrigeration (5 mg/mL concentration, 30% glycerol stock) and the enzyme has been concentrated to nearly 20 mg/mL without precipitation. DMSO stability studies have been performed and the PgFabK enzyme retains activity at DMSO concentration up to 10% (data not shown).

Protein concentrations are determined using a Bradford assay with a BSA standard rather than estimated using the theoretical extinction coefficient and A_{280} or A_{205}, due to a noted irreproducibility of the latter method with this protein (A_{280} can give PgFabK concentrations up to five times greater than the Bradford assay). We theorize that interference from the flavin prosthetic group, which absorbs UV light in the same range when in the reduced form, is the cause for this irreproducibility.

Assay optimization and kinetic characterization of recombinant PgFabK

As mentioned in the Methods section, all assay optimization and kinetic studies have been performed using the oligo-histidine-tagged enzyme. The FabK enzyme from *Streptococcus pneumoniae* has previously been isolated and characterized by Marrakchi and coworkers [16]. In these studies, SpFabK was shown to be a flavoenzyme, utilizing the FMN prosthetic group in a 1:1 stoichiometry. The *S. pneumoniae* enzyme is strongly dependent on the NADH cofactor as the hydride donor and showed no activity when NADPH was substituted for NADH. Intrinsic NADH oxidase activity in the absence of substrate was noted [16]. The apparent Km values for the crotonyl-ACP substrate and the NADH cofactor were reported to be 9 ± 1 μM (at 50 μM NADH) and 23 ± 4 μM (at 25 μM crotonyl-ACP), respectively [16]. The enzymatic reaction proceeds via a Bi-Bi double displacement (or Ping-Pong) mechanism, with the NADH cofactor binding first to the active site and reducing the FMN group, followed by displacement of NAD^+ by the enoyl substrate, which is reduced by the $FMNH_2$ group, thereby returning the enzyme to its original state [18]. Inhibitor screening studies that have been performed against the SpFabK enzyme used concentrations for crotonyl-CoA and NADH significantly greater than the reported Km values (200 μM and 400 μM, respectively) [24]. The use of balanced assay conditions, where the assay concentrations of cofactor and substrate are near their Km values, maximizes the chances of finding inhibitors with the broadest diversity in terms of mechanism of inhibition (competitive, noncompetitive, uncompetitive) [25]. In order to identify the Km values for the cofactor and substrate of *P. gingivalis* FabK, we performed a detailed kinetic analysis of the enzyme at varying concentrations of each.

We first note that the *P. gingivalis* FabK enzyme showed very little activity when attempts were made to run assays using NADH as the cofactor (very low activity seen at 400 μM, undetectable at 200 μM). However, when NADPH was substituted the enzyme showed strong activity at concentrations as low as 4 μM. Hence, unlike the SpFabK enzyme, PgFabK is dependent upon NADPH as the hydride donor in the enzymatic reaction. We also note that, similar to SpFabK, the PgFabK enzyme possesses low intrinsic NADPH oxidase activity in the absence of the crotonyl-CoA substrate. The general assay conditions, including volume, buffer conditions, enzyme and salt concentration were selected to

maximize the reaction rate as calculated by the slope (RFU/sec) of the plotted fluorescence of the NADPH cofactor. The PgFabK enzyme concentration of 30 nM was used in the experiments and was selected to allow for a steady-state time period (linear range in readings) of at least 5 minutes for each concentration of NADPH/crotonyl-CoA (Figure 4). The MOPS buffer, 50 mM, pH 7.5 was selected for use in the optimized assay due to its lower propensity for reactivity (Tris contains a potentially reactive primary amine), pH buffering range (pKa 7.2), low temperature effect on buffering capacity, low chelation effect, and low UV absorbance. A range of pH values (6.5, 7.0, 7.5, and 8.0) was tested, with 7.5 showing the greatest reaction rate (data not shown). Additionally, the stability of NADPH was a factor in the consideration of buffer choice. The degradation of NADPH is pH and temperature dependent [26]. At pH 5.0 and 30 ˚C, the half-life of NADPH is reported to be 38 minutes. The half-life is extended at higher pH and lower temperatures, and shows a half-life of 517 minutes at pH 7.0. NADPH stock solutions were prepared fresh on the days that assay experiments were run, at 1mM concentration in 50mM MOPS pH 7.5, and kept on ice. We used 100 mM NH_4Cl in all assay experiments, as this salt was previously reported to be optimal for activity and stability of the FabK enzyme [16]. We noted a complete loss of enzyme activity when the NH_4Cl was removed from the assay conditions. Interestingly, the enzyme retained activity at low (and even no) buffer concentrations, provided the salt was retained.

To calculate the apparent Km values for NADPH and the crotonyl-CoA substrate, a range of concentrations were tested for each; 11 concentrations for NADPH and 8 for crotonyl-CoA, at constant concentrations of the opposing substrate. When plots of reaction rate versus NADPH concentration (constant crotonyl-CoA concentration) were examined, a deviation from the typical kinetic behavior was immediately apparent (Figure 5, left). This atypical kinetic pattern was recognized as substrate inhibition [27]. When the concentration of NADPH was held constant and the reaction rate plotted as a function of crotonyl-CoA, there was no detectable substrate inhibition (Figure 5, right). This seems to indicate that NADPH is able to bind to the enzyme-$FMNH_2$ form of the enzyme and interfere with the binding of the enoyl substrate at high concentrations. This information is particularly relevant in the design of a balanced assay for the screening of inhibitors as well as the selection of the proper velocity equation for use in calculating Km values. It may also partly explain the intrinsic activity of the enzyme we noted above in the absence of the crotonyl-CoA substrate. The calculated reaction rates for the NADPH concentration curves (obtained from steady state slopes) were fit to Equation (1), which models substrate inhibition, while the Km values for the crotonyl substrate were derived using Equation (2). Both equations were fit using the nonlinear curve-fitting algorithm of the OriginPro v8.6 software.

The calculated apparent Km value for NADPH was 17 ± 6.5 μM (at 100 μM crotonyl-CoA), while the apparent Km of crotonyl-CoA was 48 ± 5 μM (at 50 μM NADPH). The apparent Ki value for NADPH substrate inhibition was 109 ± 45 μM (at 100 μM crotonyl-CoA). Goodness of fit was determined by analysis of reduced Chi square and adjusted R-square values, which were significant in both cases (see Table 1). The apparent Km values determined for the PgFabK cofactor and substrate are very similar to the apparent Km values reported for SpFabK, though for the substrate we used crotonyl-CoA rather than the acyl carrier protein linked, crotonyl-ACP, due to its commercial availability. It is interesting to note the higher affinity for the crotonyl substrate that the FabK enoyl-reductase enzymes (both *S. pneumoniae* and *P. gingivalis*) possess over the FabI enoyl-reductase isozyme. The reported Km value for crotonyl-CoA for the *Haemophilus influenzae* FabI was 7.3 mM [31]. The PgFabK assay conditions that were used in these studies have been optimized for low volume, high-throughput screens. All reported kinetic experiments were performed at 10 μL in 384-well, low volume plates. The Km values that have been determined for NADPH and crotonyl-CoA will be used for the concentrations of these compounds in future high-throughput screens for inhibitory agents.

Protein crystallization

In order to facilitate future structure-based drug discovery efforts against the PgFabK target, a series of protein crystallization screens were performed in an attempt to identify PgFabK crystallization conditions. Coarse-matrix crystallization screens were first performed using a variety of crystallization kits from Hampton Research (see Methods). All protein crystallization experiments were performed using the oligo-histidine-tagged enzyme. Initial attempts used PgFabK at a concentration of 10 mg/mL in MOPS buffer (10 mM, pH 7.5) with 100mM NH_4Cl and 5 mM DTT, as similar conditions had been previously reported for SpFabK [23], however because a large degree of protein precipitation was seen at this concentration, we modified the conditions to use PgFabK at 5 mg/mL. The hanging-drop, vapor diffusion method was used, with two trial drops per well. One drop contained protein without NADPH cofactor or substrate, while the other contained excess NADPH. Initial screens were set up in duplicate for two temperature conditions, 25 ˚C and 4 ˚C.

Crystal growth was noted within one week for several conditions at 25 ˚C and 4 ˚C, with little dependence of crystal growth on temperature. The most promising crystals (by size and morphology) grew out from PEG/Ion (#46), which is 0.2 M Na citrate and 20% w/v PEG 3350. Large, yellow needles, single or twinned, grew in both the apo protein and NADPH-protein drops, though the size and quality of

the crystals appeared better in the NADPH condition (by visual inspection). A variety of other hit conditions were identified, typically involving a citrate, tartrate, or malonate salt with 20% PEG 3350. Another promising hit condition was found in Crystal Screen 2 (#14), which is 0.1 M Na citrate, 0.2 M K Na tartrate, and 2 M NH_4SO_4. Crystals were harvested from both conditions, looped through 50% glycerol (with well buffer) for cryoprotection, and screened for ability to diffract x-rays using an in-house x-ray diffractometer. Unfortunately, neither condition produced crystals that diffracted to a suitable resolution for data collection (7 - 8 Å resolution).

In an attempt to identify crystallization conditions leading to improved crystal diffraction, we performed a series of microseeding trials (see Methods). Microseed matrix screening techniques have been shown to be capable of identifying novel protein crystallization conditions leading crystals with significantly better diffraction [32]. Two conditions were identified using this technique against the Index screen (#56 & #87) that yielded crystals of sufficient size and quality for diffraction studies (Figure 6). In both cases, the crystals were identified in drops containing excess NADPH. Crystals from Index #87 (0.2 Na malonate, pH 7.0, 20% PEG 3350) were harvested, looped through 50% glycerol for cryoprotection, and cooled to 100 ˚K for data collection. The crystals diffracted to 1.9 Å resolution and two data sets were collected at 21-ID-G, LS-CAT, sector 21, at the Advanced Photon Source, Argonne National Laboratory (Figure 7). The structural determination of PgFabK using molecular replacement is now in progress.

Conclusions

Enoyl-ACP reductase II, FabK, is an essential enzyme in the bacterial fatty acid synthesis pathway and a potentially important infectious disease drug target. We have cloned, expressed, purified and characterized the FabK enzyme from *Porphyromonas gingivalis*, a key causative organism in chronic periodontitis. PgFabK is the second FabK enzyme to be characterized, after *Streptococcus pneumoniae* FabK. FabK is an FMN flavoenzyme whose enzymatic reaction proceeds via a Bi-Bi, double displacement (ping-pong) mechanism. The cloning and expression protocols that have been presented involved standard methods and did not require any major troubleshooting. The purification protocol involves two steps of chromatography and yields 10 - 15 mg per liter of highly purified protein (1.2 - 1.9 mg of purified protein per gram of wet weight cells), on average, with greater than 98% purity, which is sufficient for crystallographic experiments. Unlike its counterpart from *S. pneumoniae*, which has previously been characterized, PgFabK was shown here to rely on NADPH rather than NADH as the

hydride donating cofactor. Interestingly, we noted during our enzyme kinetics experiments that the NADPH cofactor was able to inhibit the reaction at high concentrations. This observed substrate inhibition was not previously reported for NADH and SpFabK.

The ultimate goal of the studies presented here was the characterization of the enzyme for future drug discovery efforts, including high-throughput screening and structure-based drug discovery. To that end, we have experimentally determined the Km values of the cofactor, NADPH, and substrate, crotonyl-CoA, so that balanced assay conditions could be identified. We have carefully optimized the assay conditions for low-volume, high-throughput compound screening. The 10 µL assay volume that we have optimized for 384-well screening in-house can be easily translated to 1536-well format for use in external screening campaigns. Additionally, to advance our structure-based discovery goals, we have identified crystallization conditions using microseeding methods that resulted in PgFabK protein crystals that diffracted very well. We are currently working on the solution of the structure using molecular replacement with the previously published structure of SpFabK. We believe that the work presented here will greatly facilitate drug discovery efforts directed toward the prevention and treatment of chronic periodontitis and the methods presented can be easily translated toward the expression, purification and characterization of the FabK enzyme from other bacterial species of clinical interest.

Acknowledgements

Support for this research was provided by the UIC College of Dentistry MOST program, NIH T32DE018381. The authors wish to acknowledge the assistance of Dr. Hyun Lee with the manuscript preparation and proofing. Use of the Advanced Photon Source was supported by the U. S. Department of Energy, Office of Science, Office of Basic Energy Sciences, under Contract No. DE-AC02-06CH11357. Use of the LS-CAT Sector 21 was supported by the Michigan Economic Development Corporation and the Michigan Technology Tri-Corridor for the support of this research program (Grant 085P1000817).

References

[1] L.J. Jin, G.C. Armitage, B. Klinge, N.P. Lang, M. Tonetti, R.C. Williams, Global oral health inequalities: task group--periodontal disease. Adv Dent Res 23 (2011) 221-226.

[2] C.B. Snowden, T.R. Miller, A.F. Jensen, B.A. Lawrence, Costs of medically treated craniofacial conditions. Public Health Rep 118 (2003) 10-17.

[3] A. Savage, K.A. Eaton, D.R. Moles, I. Needleman, A systematic review of definitions of periodontitis and methods that have been used to identify this disease. J Clin Periodontol 36 (2009) 458-467.

[4] M. Avila, D.M. Ojcius, O. Yilmaz, The oral microbiota: living with a permanent guest. DNA and cell biology 28 (2009) 405-411.

[5] J.M. Lovegrove, Dental plaque revisited: bacteria associated with periodontal disease. J N Z Soc Periodontol (2004) 7-21.

[6] N.G. Chavarry, M.V. Vettore, C. Sansone, A. Sheiham, The relationship between diabetes mellitus and destructive periodontal disease: a meta-analysis. Oral Health Prev Dent 7 (2009) 107-127.

[7] S.G. Fitzpatrick, J. Katz, The association between periodontal disease and cancer: A review of the literature. J Dent (2009).

[8] K. Joshipura, J.C. Zevallos, C.S. Ritchie, Strength of evidence relating periodontal disease and atherosclerotic disease. Compend Contin Educ Dent 30 (2009) 430-439.

[9] G. Hajishengallis, S. Liang, M.A. Payne, A. Hashim, R. Jotwani, M.A. Eskan, M.L. McIntosh, A. Alsam, K.L. Kirkwood, J.D. Lambris, R.P. Darveau, M.A. Curtis, Low-abundance biofilm species orchestrates inflammatory periodontal disease through the commensal microbiota and complement. Cell Host Microbe 10 (2011) 497-506.

[10] A. Japoni, A. Vasin, S. Noushadi, F. Kiany, S. Japoni, A. Alborzi, Antibacterial susceptibility patterns of *Porphyromonas gingivalis* isolated from chronic periodontitis patients. Medicina oral, patologia oral y cirugia bucal 16 (2011) e1031-1035.

[11] C.M. Ardila, M.I. Granada, I.C. Guzman, Antibiotic resistance of subgingival species in chronic periodontitis patients. J Periodontal Res 45 (2010) 557-563.

[12] A. Blinkhorn, P.M. Bartold, M.P. Cullinan, T.E. Madden, R.I. Marshall, S.L. Raphael, G.J. Seymour, Is there a role for triclosan/copolymer toothpaste in the management of periodontal disease? Br Dent J 207 (2009) 117-125.

[13] Y. Vered, A. Zini, J. Mann, W. DeVizio, B. Stewart, Y.P. Zhang, L. Garcia, Comparison of a dentifrice containing 0.243% sodium fluoride, 0.3% triclosan, and 2.0% copolymer in a silica base, and a dentifrice containing 0.243% sodium fluoride in a silica base: a three-year clinical trial of root caries and dental crowns among adults. J Clin Dent 20 (2009) 62-65.

[14] H. Lu, P.J. Tonge, Inhibitors of FabI, an enzyme drug target in the bacterial fatty acid biosynthesis pathway. Acc Chem Res 41 (2008) 11-20.

[15] J.A. Karlowsky, N. Kaplan, B. Hafkin, D.J. Hoban, G.G. Zhanel, AFN-1252, a FabI inhibitor, demonstrates a *Staphylococcus*-specific spectrum of activity. Antimicrob Agents Chemother 53 (2009) 3544-3548.

[16] H. Marrakchi, W.E. Dewolf, Jr., C. Quinn, J. West, B.J. Polizzi, C.Y. So, D.J. Holmes, S.L. Reed, R.J. Heath, D.J. Payne, C.O. Rock, N.G. Wallis, Characterization of *Streptococcus pneumoniae* enoyl-(acyl-carrier protein) reductase (FabK). Biochem J 370 (2003) 1055-1062.

[17] R.J. Heath, J. Li, G.E. Roland, C.O. Rock, Inhibition of the *Staphylococcus aureus* NADPH-dependent enoyl-acyl carrier protein reductase by triclosan and hexachlorophene. J Biol Chem 275 (2000) 4654-4659.

[18] J. Saito, M. Yamada, T. Watanabe, M. Iida, H. Kitagawa, S. Takahata, T. Ozawa, Y. Takeuchi, F. Ohsawa, Crystal structure of enoyl-acyl carrier protein reductase (FabK) from *Streptococcus pneumoniae* reveals the binding mode of an inhibitor. Protein Sci 17 (2008) 691-699.

[19] H. Marrakchi, Y.M. Zhang, C.O. Rock, Mechanistic diversity and regulation of type II fatty acid synthesis. Biochem Soc Trans 30 (2002) 1050-1055.

[20] R.P. Massengo-Tiasse, J.E. Cronan, *Vibrio cholerae* FabV defines a new class of enoyl-acyl carrier protein reductase. J Biol Chem 283 (2008) 1308-1316.

[21] K.E. Nelson, R.D. Fleischmann, R.T. DeBoy, I.T. Paulsen, D.E. Fouts, J.A. Eisen, S.C. Daugherty, R.J. Dodson, A.S. Durkin, M. Gwinn, D.H. Haft, J.F. Kolonay, W.C. Nelson, T. Mason, L. Tallon, J. Gray, D. Granger, H. Tettelin, H. Dong, J.L. Galvin, M.J. Duncan, F.E. Dewhirst, C.M. Fraser, Complete genome sequence of the oral pathogenic bacterium *Porphyromonas gingivalis* strain W83. Journal of bacteriology 185 (2003) 5591-5601.

[22] M.M. Bradford, A rapid and sensitive method for the quantitation of microgram quantities of protein utilizing the principle of protein-dye binding. Anal Biochem 72 (1976) 248-254.

[23] J. Saito, M. Yamada, T. Watanabe, H. Kitagawa, Y. Takeuchi, Crystallization and preliminary X-ray analysis of enoyl-acyl carrier protein reductase (FabK) from *Streptococcus pneumoniae*. Acta Crystallogr Sect F Struct Biol Cryst Commun 62 (2006) 576-578.

[24] S. Takahata, M. Iida, Y. Osaki, J. Saito, H. Kitagawa, T. Ozawa, T. Yoshida, S. Hoshiko, AG205, a novel agent directed against FabK of *Streptococcus pneumoniae*. Antimicrob Agents Chemother 50 (2006) 2869-2871.

[25] J. Yang, R.A. Copeland, Z. Lai, Defining balanced conditions for inhibitor screening assays that target bisubstrate enzymes. J Biomol Screen 14 (2009) 111-120.

[26] J.T. Wu, L.H. Wu, J.A. Knight, Stability of NADPH: effect of various factors on the kinetics of degradation. Clinical chemistry 32 (1986) 314-319.

[27] M.C. Reed, A. Lieb, H.F. Nijhout, The biological significance of substrate inhibition: a mechanism with diverse functions. BioEssays : news and reviews in molecular, cellular and developmental biology 32 (2010) 422-429.

[28] D. Marquardt, An algorithm for least-squares estimation of nonlinear parameters. SIAM Journal on Applied Mathematics 11 (1963) 431-444.

[29] R.J. Leatherbarrow, Enzfitter. A non-linear regression data analysis program for the IBM PC, Elsevier Science Publishers BV, Amsterdam, 1987.

[30] F. Mosteller, J.W. Tukey, Data analysis and regression : a second course in statistics., Addison Wesley, 1977.

[31] J. Marcinkeviciene, W. Jiang, L.M. Kopcho, G. Locke, Y. Luo, R.A. Copeland, Enoyl-ACP reductase (FabI) of *Haemophilus influenzae*: steady-state kinetic mechanism and inhibition by triclosan and hexachlorophene. Arch Biochem Biophys 390 (2001) 101-108.

[32] G.C. Ireton, B.L. Stoddard, Microseed matrix screening to improve crystals of yeast cytosine deaminase. Acta Crystallogr D Biol Crystallogr 60 (2004) 601-605.

Figure Legends

Figure 1. PCR gel analysis. The 942 kb PgFabK PCR product, 50 µL production, performed in duplicate, is shown on 1% agarose gel.

Figure 2. PgFabK expression analysis. Protein expression levels at four hours post-induction. 1.0 mM IPTG, lanes 1a - 1d; 0.5 mM IPTG, lanes 2a - 2d; 0.25 mM IPTG, lanes 3a - 3d. Soluble, non-induced fractions, lanes Xa; Soluble, induced fractions, lanes Xb; insoluble, non-induced fractions, lanes Xc; insoluble, induced, lanes Xd.

Figure 3. PgFabK purification analysis. Lane 1, sample in lysis buffer, prior to sonication; Lane 2, crude lysate, prior to centrifugation; Lanes 3, crude extract, prior to filtration; Lane 4, clarified extract; Lane 5, pellet sample, insoluble fraction; Lane 6, Ni column flow through; Lane 7, Ni column, collected fractions, pooled; Lane 8, Gel Filtration column, collected fractions, pooled.

Figure 4. The PgFabK fluorescence intensity assay. The assay shows a decrease in the fluorescence intensity (ex 340, em 460nm) of NADPH over time (triplicate). The NADPH concentration is 8.8 µM and the crotonyl-CoA concentration is 26 µM.

Figure 5. PgFabK rate vs. substrate concentration. A. A plot of the PgFabK enzyme rate (RFU/sec) with crotonyl-CoA concentration held at 100 µM and varying concentrations of NADPH reveals a pattern typical of substrate inhibition. B. A plot of the PgFabK enzyme rate (RFU/sec) with NADPH concentration held at 50 µM and varying concentrations of crotonyl-CoA shows a typical rate pattern.

Figure 6. PgFabK crystals. The final crystal growth conditions were 0.2M Na malonate, pH 7.0, 20% PEG 3350, 5mg/mL protein in drops 1:1 (2 µL each) with well buffer & 1 µL microseed stock solution.

Figure 7. PgFabK crystal diffraction. The x-ray diffraction pattern of PgFabK crystals shows diffraction to 1.9Å resolution.

Table Titles

Table 1. Purification of PgFabK, enoyl-ACP reductase II

Table 2. Fitted kinetic parameters and statistics of fit

Figures

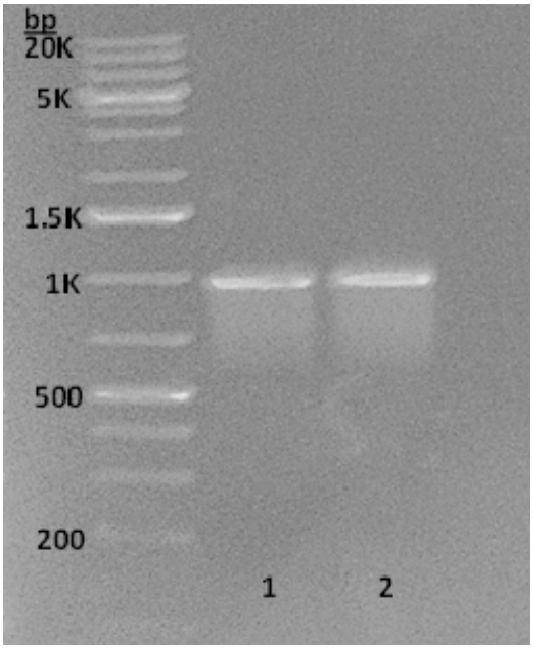

Figure 1. PCR gel analysis. The 942 kb PgFabK PCR product, 50 µL production, performed in duplicate, is shown on 1% agarose gel.

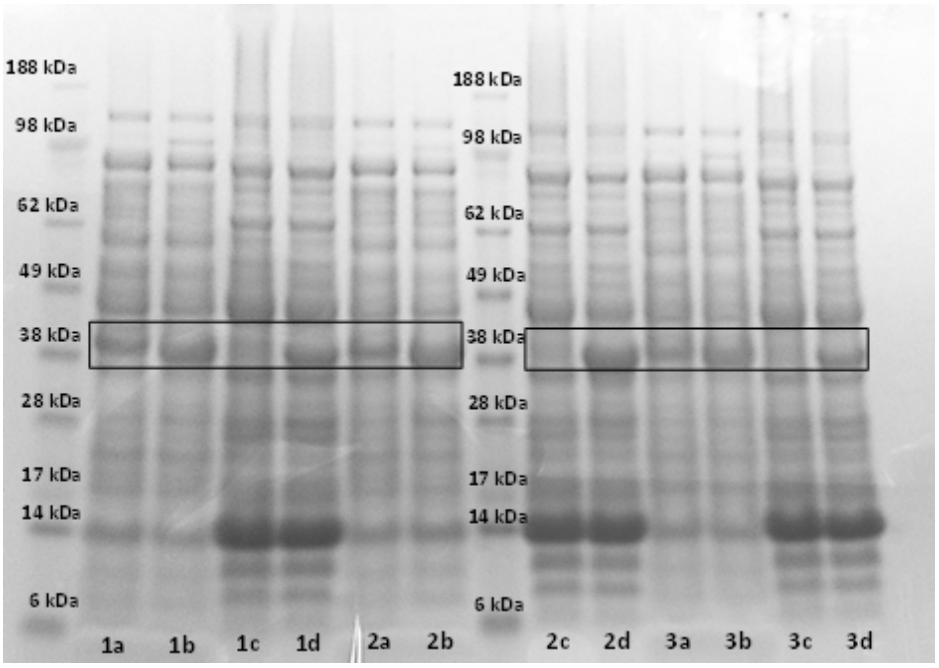

Figure 2. PgFabK protein mini-expression analysis. Protein expression levels at four hours post-induction. 1.0 mM IPTG, lanes 1a - 1d; 0.5 mM IPTG, lanes 2a - 2d; 0.25 mM IPTG, lanes 3a - 3d. Soluble, non-induced fractions, lanes Xa; Soluble, induced fractions, lanes Xb; insoluble, non-induced fractions, lanes Xc; insoluble, induced, lanes Xd.

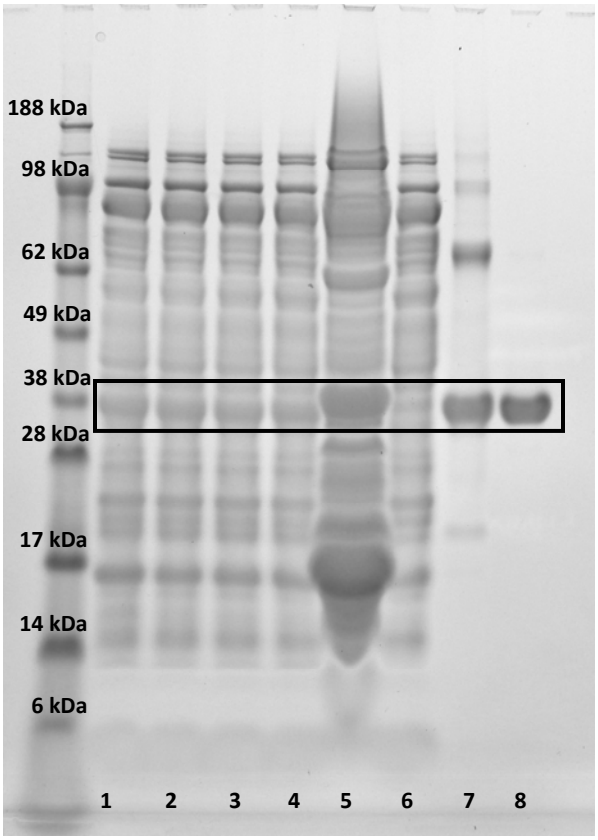

Figure 3. PgFabK purification analysis. Lane 1, sample in lysis buffer, prior to sonication; Lane 2, crude lysate, prior to centrifugation; Lanes 3, crude extract, prior to filtration; Lane 4, clarified extract; Lane 5, pellet sample, insoluble fraction; Lane 6, Ni column flow through; Lane 7, Ni column, collected fractions, pooled; Lane 8, Gel Filtration column, collected fractions, pooled.

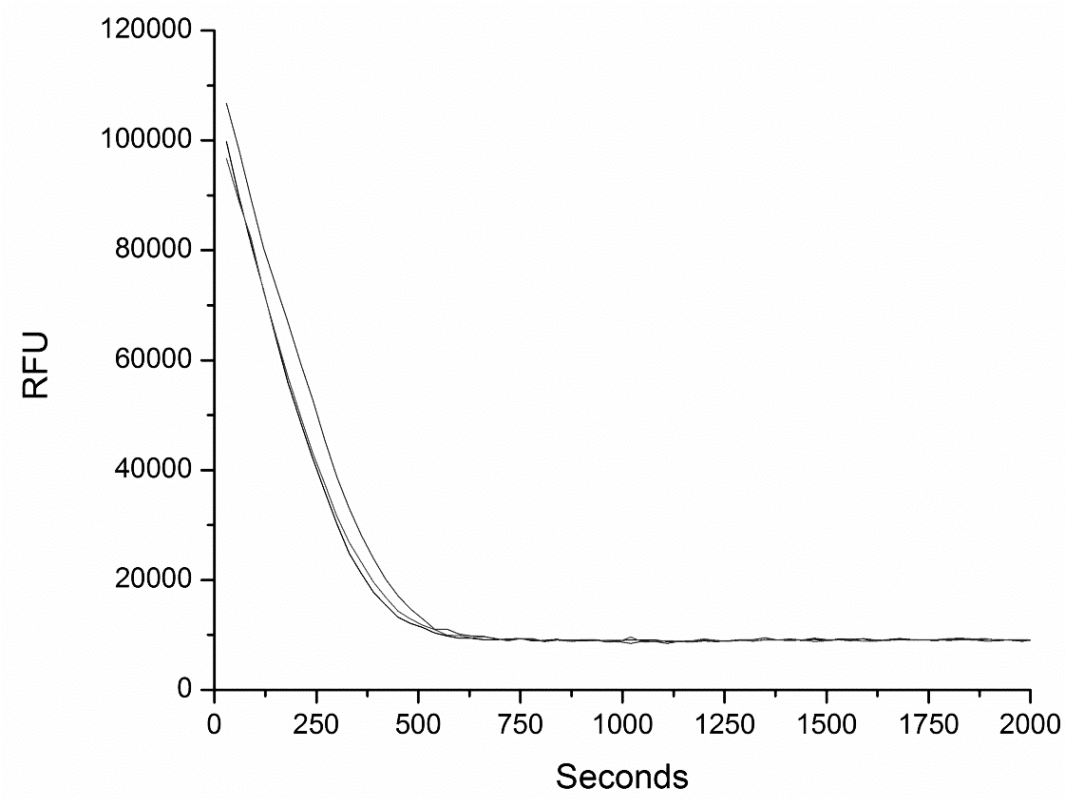

Figure 4. The PgFabK fluorescence intensity assay. The assay shows a decrease in the fluorescence intensity (ex 340, em 460nm) of NADPH over time (triplicate). The NADPH concentration is 8.8 μM and the crotonyl-CoA concentration is 26 μM.

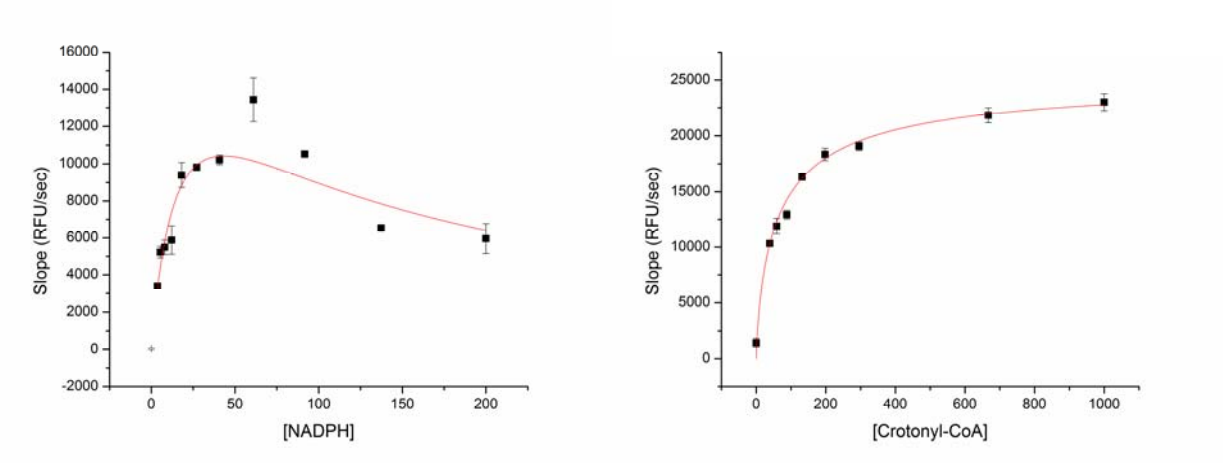

Figure 5. PgFabK Rate vs. Substrate Concentration. A. A plot of the PgFabK enzyme rate (RFU/sec) with crotonyl-CoA concentration held at 100 µM and varying concentrations of NADPH reveals a pattern typical of substrate inhibition. **B**. A plot of the PgFabK enzyme rate (RFU/sec) with NADPH concentration held at 50 µM and varying concentrations of crotonyl-CoA shows a typical rate pattern.

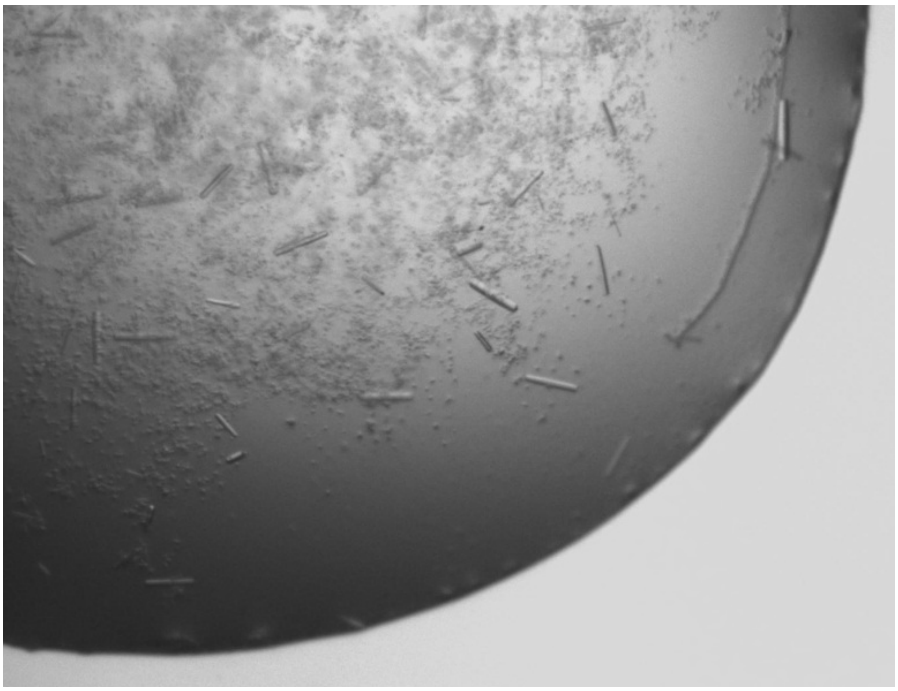

Figure 6. PgFabK crystals. The final crystal growth conditions were 0.2M Na malonate, pH 7.0, 20% PEG 3350, 5mg/mL protein in drops 1:1 (2 µL each) with well buffer & 1 µL microseed stock solution.

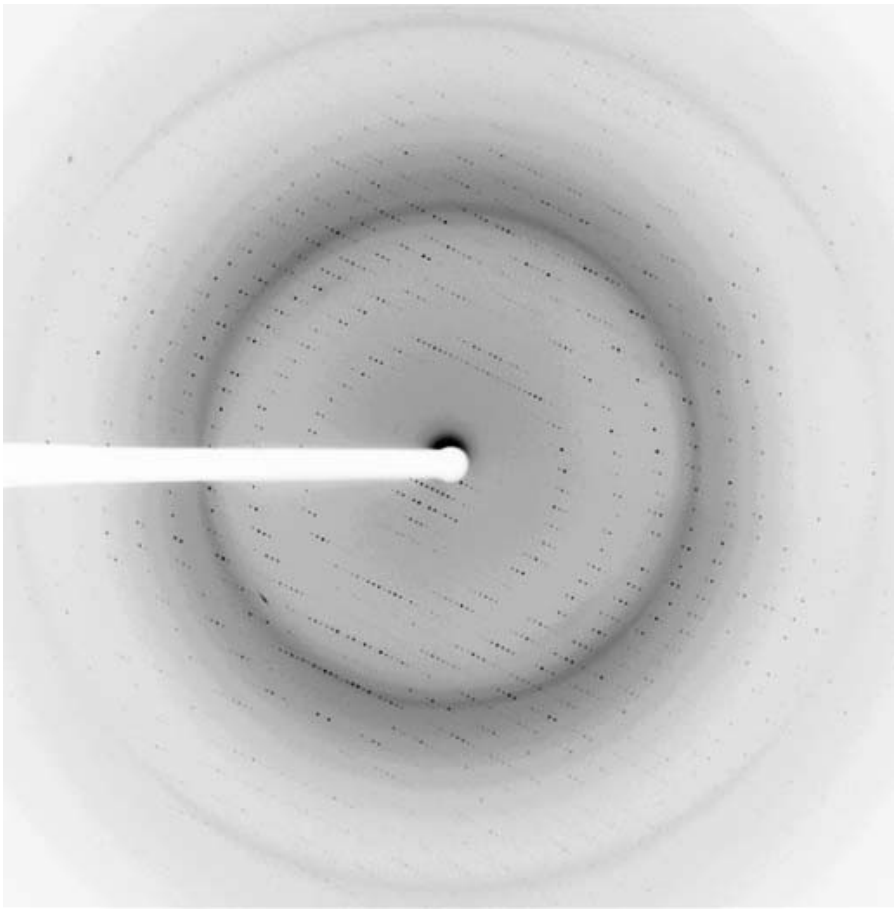

Figure 7. PgFabK crystal diffraction. The x-ray diffraction pattern of PgFabK crystals shows diffraction to 1.9Å resolution.

Tables

Table 1. Purification of PgFabK, enoyl-ACP reductase II

Step	Volume (ml)	Concentration (mg/ml)	Total Protein (mg)	Total Enzyme Activity[1] (μmol/min)	Specific Activity (μmol/min/mg)	K_{cat} (s^{-1})	Yield (%)	Purity (%)
Crude Extract	123	3.8	467.4	0.028	0.74	0.37	100	14
After Ni IMAC	48	0.55	26.4	0.025	4.53	2.28	34.6	86
After G.F.	34	0.45	15.3	0.024	5.25	2.65	23.2	100

Purification was achieved from 3 x 500 ml culture of *E. coli* BL21 (DE3), 8.2 gm wet weight cells, as discussed in Methods.

[1] Enzyme activity was measured by monitoring decrease in NADPH A_{340} in 1-ml cuvettes, 10 μL protein, 50 μM crotonyl-CoA, 50 μM NADPH, 50 μM MOPS pH 7.5, 100 μM NH_4Cl. Extinction coefficient (ε) of NADPH at 340 nM is 6220 M^{-1} cm^{-1}.

Table 2. Fitted kinetic parameters and statistics of fit

Name	Value	Standard Error	Reduced Chi-squared	Adusted R-squared
Km (NADPH)	17.1	6.59	16.1	0.92
Ki (NADPH)	109.5	44.7	16.1	0.92
Km (crotonyl-CoA)	47.8	5.14	5.62	0.98